International Conference on Global Optimization and Its Applications 2022 (ICoGOIA 2022), Melaka, November 19-20, 2022

Dielectric and mechanical properties of zirconium silicate and polyurethane dielectric elastomer composite

Muhammad Naiem Naqiuddin b Zaharin[1*], Ku Ahmad, K.Z[1*], R N Othman[1], Yahaya, R[2]

[1] Engineering Faculty, Universiti Pertahanan Nasional Malaysia, MALAYSIA.
[2] Science and Technology Research Institute of Defence (STRIDE), MALAYSIA

**Corresponding author email: kuzarina@upnm.edu.my , naiemnaqiuddin@gmail.com*

Abstract

Polyurethane (PU) is an interesting polymer that possesses excellent high dielectric permittivity, low dielectric loss, and great flexibility, which makes it promising to be applied as a dielectric elastomer generator (DEG). However, enhancement in terms of dielectric permittivity is still necessary to ensure PU practicability in the industry. In this paper, a high permittivity ceramic nanofiller, zirconium silicate ($ZrSiO_4$), was incorporated with a PU matrix to fabricate a composite elastomer. $ZrSiO_4$ nanofillers and PU matrix were synthesized through the melt-mixing method at various weight percentages (10 wt.%, 20 wt.%, 30 wt.%, 40 wt.%, and 50 wt.%). Fourier Transform Infrared Spectroscopy (FTIR) was used to investigate the structural characteristic of the composite. The dielectric and mechanical characterization of the composites was also been studied. The results from FTIR indicate that the $ZrSiO_4$ nanofillers were successfully synthesized within the PU matrix. Other than that, at 50 wt.% of $ZrSiO_4$, the PU/$ZrSiO_4$ recorded dielectric permittivity up to 12.07 (33.5% higher than pristine PU) while maintaining low dielectric loss and low conductivity. The ultimate tensile stress and elongation at the break of the PU composites were affected by the increment of $ZrSiO_4$ contents but they still maintained excellent mechanical attributes. These PU/$ZrSiO_4$ composites have the potential to be used as dielectric elastomers in the DEG application.

Keywords: Polyurethane, Dielectric elastomer, Zirconium Silicate, Electrical properties, Polymer matrix composites

1. Introduction

Dielectric elastomers (DE), a novel type of electro-active polymers, were first identified in the 1990s. The early discovery of dielectric elastomers was greatly aided by research into electrostrictive polymers and a keen interest in robotics. The conclusion and proof that actuation utilizing polymers with Maxwell's stress alone was an interesting option for actuation was then presented at the SRI International conference by Pelrine and others (Pelrine & Kornbluh, 2008). Numerous studies on dielectric elastomers have already been conducted since then.

The industry's capacity to use dielectric elastomers is still up for debate. Because of this, much research has been done over the years in the areas of material synthesis and optimization to create a DE that can meet the demands of the application. Beginning in the late 2000s, researchers have often employed polymers with functionalized nanofiller to develop dielectric elastomers in order to accomplish specific objectives like high dielectric permittivity, superior breakdown strength, high actuation strain, etc. (Liu et al., 2009; Zhang et al., 2008, 2009). Dielectric elastomers continue to draw interest from researchers 30 years after their first discovery due to their innovative optimization techniques and wide range of possible uses.

This study cooperates polyurethane (PU) matrix and zirconia silicate ($ZrSiO_4$) to develop a DE with excellent dielectric and mechanical properties. PU possesses high dielectric permittivity (~8), low dielectric loss, and super elongation, making it very suitable to be applied as DEG (Brochu & Pei, 2010). $ZrSiO_4$ possesses high dielectric permittivity and it is abundant, making it a very cost-effective filler (Varghese et al., 2011). The preparation of PU/$ZrSiO_4$ elastomer is described in this paper. The morphology, dielectric and mechanical properties of the PU/$ZrSiO_4$ composite were investigated and analyzed for DEG application.

2. Literature Review

DE is a type of electroactive polymer (EAP) that exhibits deformation with the presence of an electric field. It possesses superiorities such as lightweight, large deformation, high energy density, rapid response, and ease of processing (Gao et al., 2021). It can convert electrical energy into mechanical energy, and vice versa, making it suitable to be applied as both an actuator and a generator. The capacitive of DE is changeable, by manipulating the dielectric permittivity and mechanical properties of the elastomer, as shown in Eq. 1. In that equation, ε_o represents permittivity of free space, ε_r represents dielectric permittivity of the material, A represents the elastomer surface area and z represents the elastomer thickness.

$$C = \varepsilon_o \varepsilon_r \frac{A}{z} \tag{1}$$

One of the applications of DE is a dielectric elastomer generator (DEG), where the elastomer converts the oscillating mechanical power into usable electrical energy. The working principle of DEG is illustrated in Figure 1 and described in Table 1. Based on the working principle, it is understandable that the performance of DEG relies on the dielectric and mechanical properties of the elastomer. The DEG needs to possess high dielectric permittivity, and also high elongation at break in order to harvest high electrical energy. The net amount of harvested energy can be calculated using Eq. 2, where U represents the harvested energy, C represents the capacitance of the elastomer, V represents the induced voltage, and 1 and 2 represent the relaxed and stretched state, respectively.

$$U = \frac{1}{2} C_2 V_2^2 - \frac{1}{2} C_1 V_1^2 \tag{2}$$

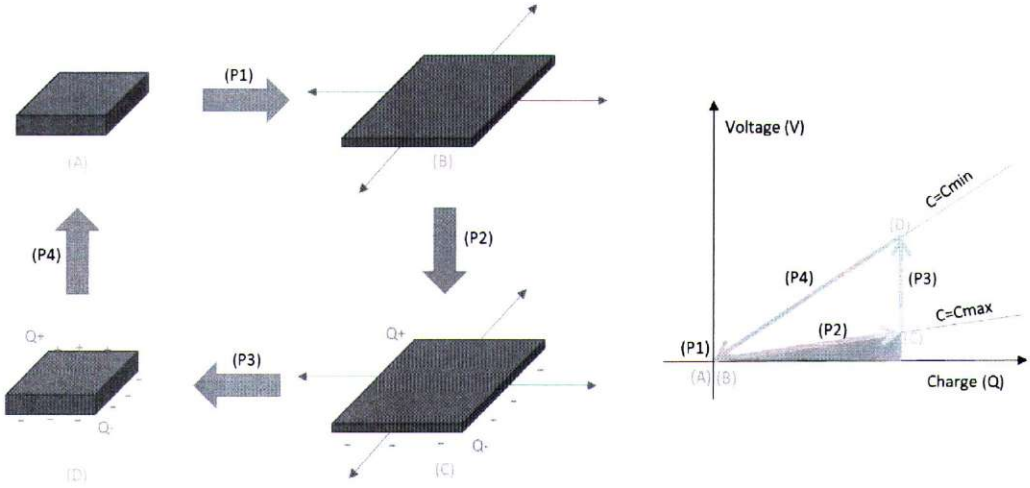

Figure 1 Illustration of DEG working principle

Table 1 Description of DEG working principle

Phase	Description
Phase 1 (P1)	As the DEG initially dwells in a relaxed state (A), where its capacitance is minimum, external loads make it expand and lead it to stretched state (B), where the capacitance is maximum. No charge is present on the DEG during this phase
Phase 2 (P2)	Charge Q is deposited on the electrodes, leading the DEG into a charged state (C), where the capacitance is the same as in state (B). This phase is called "priming," and it involves an amount of electrical energy being spent to charge the device
Phase 3 (P3)	As the charge on the DEG is held constant, the external loads and the DE elastic stresses make work against the electrostatic charge, taking the DEG back to a state (D) with minimum capacitance, Cmin. During this generation phase, the external forces are converted into electrostatic energy and stored in the DEG electric field
Phase 4 (P4)	The DEG is finally held in the minimum capacitance configuration and discharged, and the stored electrostatic energy is harvested. The net amount of generated electrical energy is the difference between the energy recovered during the discharging phase (P4), and that spent during priming (P1)

Of late, researchers had investigated a few methods to enhance the dielectric properties of DE. One of the methods is by incorporating ceramics fillers into the polymer matrix. This type of filler usually possesses high dielectric permittivity, which provides it with the ability to enhance the dielectric permittivity of the elastomer. However, this type of nanofillers needs high loadings to be effective, which leads to the deterioration of the elastomer's flexibility (Wan et

al., 2018). Luo and his team (2022) recently synthesized polydopamine (PDA) modified 1D barium titanate (BT@PDA) nanofibers with thermoplastic polyurethane (TPU) to fabricate a DE with high sensitivity (Luo et al., 2022). The results show that 10 wt.% of BT@PDA can enhance TPU dielectric constant up to 6.97 at 1 kHz. However, the elongation of the composite deteriorates, due to a large number of fibers, limiting the deformation of the rubber. Yang et al (2019) also synthesized 4,4′-diphenylmethane diisocyanate (MDI) modified BT fillers into TPU and the results show that the dielectric permittivity of TPU enhanced with the presence of BT fillers, but the mechanical properties of the elastomer were also depreciated (Yang et al., 2019). Other ceramic nanofillers were proven to execute identical results such as titanium dioxide (TiO_2) (He et al., 2020), and strontium titanate ($SrTiO_3$) (Namitha & Sebastian, 2017).

3. Materials and Methods

3.1. Materials

The polyurethane (PU) granules, Zirconia (IV) Silicate ($ZrSiO_4$) powder, and N-methyl-2-pyrrolidone (NMP) solvent were acquired from Sigma-Aldrich and used without further purification.

3.2. Preparation of the PU/$ZrSiO_4$ composites

The desired amount of $ZrSiO_4$ nanoparticles (refer Table 2) was dispersed in 100 mL of NMP under sonication for 30 minutes, followed by adding 15g of PU and stirring the mixture mechanically for three hours at 150 rpm and 140°C. The mixture was poured into the glass mold and dried in an 80°C oven for 16 hours to eliminate all solvents. All the casted films then were removed from the mold. The films were then labelled as PU/ $ZrSiO_4$-x, where x represents the weight percentage of $ZrSiO_4$ nanoparticles.

Table 2 Amount of material used for each sample

Material	PU/ $ZrSiO_4$-10wt.%	PU/ $ZrSiO_4$-20wt.%	PU/ $ZrSiO_4$-30wt.%	PU/ $ZrSiO_4$-40wt.%	PU/ $ZrSiO_4$-50wt.%
PU	15g	15g	15g	15g	15g
$ZrSiO_4$	1.5g	3g	4.5g	6g	7.5g

3.3. Characterization

The composition of the PU, $ZrSiO_4$ and PU/$ZrSiO_4$-50wt.% composite was characterized using FTIR at spectra between 4000 and 400 cm^{-1}. The dielectric properties of the composites at different weight percentage of $ZrSiO_4$ were measured using an impedance analyzer (4294A, Agilent Technologies) in a frequency range of 30 Hz to 120 MHz at room temperature. The mechanical properties of the composite at different weight percentage of $ZrSiO_4$ were tested through a tensile test using Instron Universal Testing Machine according to ISO 37:2017 standard. The microstructural of PU/$ZrSiO_4$-20wt.% and PU/$ZrSiO_4$-50wt.% composites were characterized by high resolution field emission scanning electron microscope solutions (FESEM) (ZEISS GeminiSEM 500) and the elemental composition of both composites were mapped using Energy Dispersive X-Ray analysis (EDX).

4. Results and Discussion

The FTIR spectra of PU, $ZrSiO_4$ and PU/$ZrSiO_4$-50wt.% are shown in Figure 2. The absorbance at ~3335 cm–1 is consistent with the stretching of the NH bond and is characteristic of the urethane and urea groups. The other characteristic bands are ~2900 cm–1 due to the alkane -CH stretching vibration, 1174 cm–1 due to the coupled C-N and C-O stretching vibrations, and 1062 cm–1 due to the ester C-O-C symmetric stretching vibration (Dias et al., 2010). The bands at ~431 and ~860 cm-1, which appear in the spectrum of $ZrSiO_4$ nanoparticles can be attributed to asymmetric bending vibration and stretching vibration of Si–O–Si bonds, respectively, while the band at ~650 cm-1 can be attributed to Zr–O stretching vibrations (Musyarofah et al., 2019; Nandiyanto et al., 2019). The presence of these bands in PU/ $ZrSiO_4$ composite indicates that the $ZrSiO_4$ nanofillers are well dispersed in the PU matrix. All characteristic peaks are summarized in Table 3. There is no new band or peak presence in any composite samples, indicating there was no chemical reaction between PU and $ZrSiO_4$.

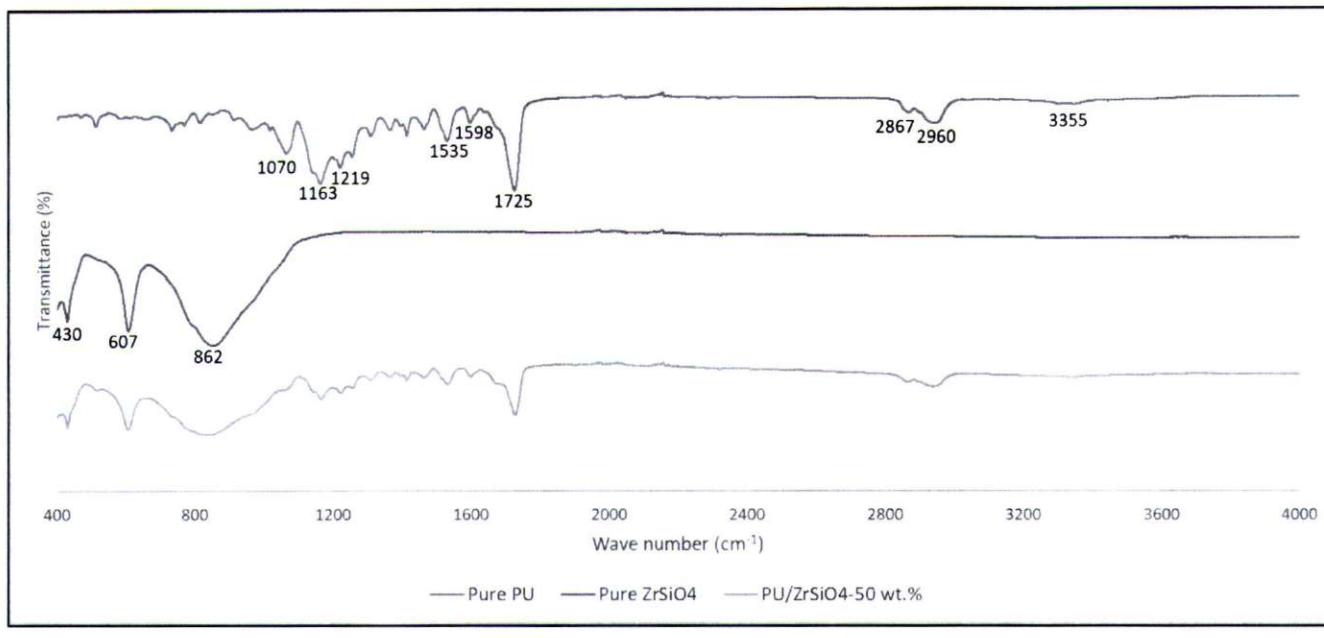

Figure 2 FTIR spectra of PU, $ZrSiO_4$ nanofillers and PU/$ZrSiO_4$-50 wt.% composite

Table 3 FTIR characteristic band of PU, $ZrSiO_4$ and PU/$ZrSiO_4$-50 wt.% composite

Frequency (cm^{-1})	Assignment
3050-3750	NH stretching vibration
2800-3000	CH stretching vibration: anti-symmetric and symmetric stretching vibration mode
1600-1800	Amide I: C=O stretching vibration
1500-1540	Amide II: C-N stretching
1200-1289	Amide III: in-plane N-H formation
1070-1074	C-N stretch
860	Stretching vibration of Si–O–Si
650	Zr–O stretching vibrations
431	Bending vibration of Si–O–Si

Figure 3 shows the dielectric permittivity of PU and PU/$ZrSiO_4$ composite. The dielectric permittivity of the PU composite shows an increment with the presence of $ZrSiO_4$ up to 33.5% for the composite with 50 wt.% of $ZrSiO_4$ compared to pure PU at 1kHz. The presence of nanofillers within the PU polymer increases the interfacial polarization of the elastomer. The electrostatic polarization at the nanoparticles interface leads to the field-induced polarization of the dispersed phase relative to the continuous phase. The positive and negative charges appear at the surface of the particles when an electric voltage is applied, creating dipoles, as illustrated in Figure 4. The charges align head-to-tail in the direction of the electric field and polarization leads to the increased capability of the prepared dielectric materials to store energy (Stiubianu et al., 2015).

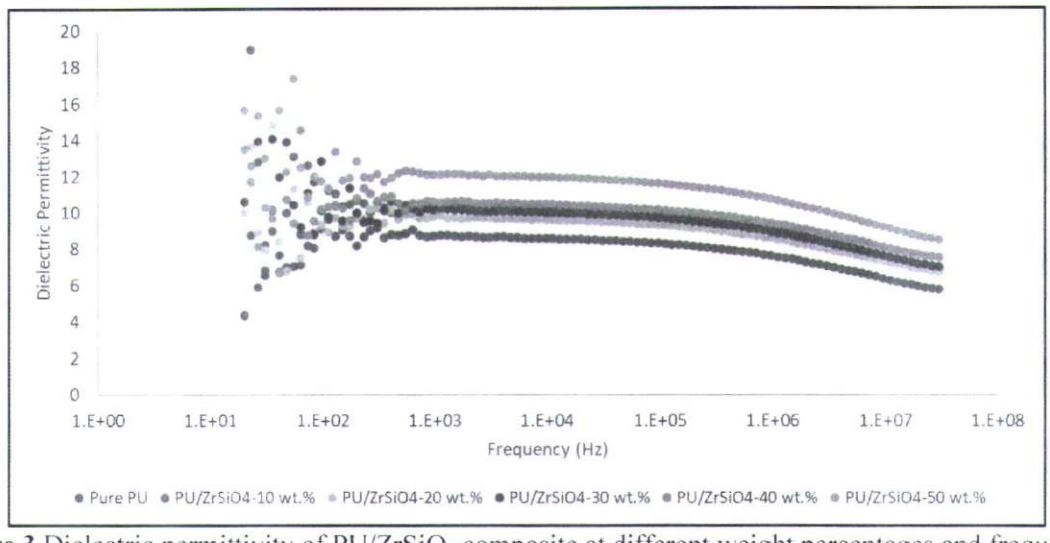

Figure 3 Dielectric permittivity of PU/$ZrSiO_4$ composite at different weight percentages and frequencies

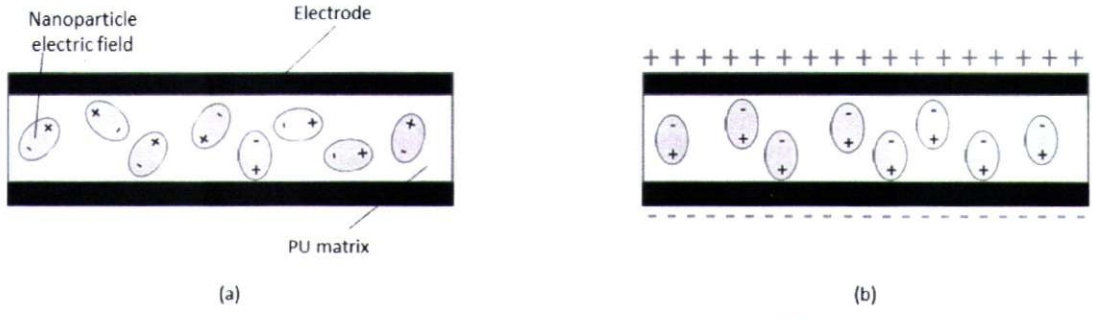

Figure 4 Schematic illustration of field-induced polarization (a) with OFF voltage, (b) with ON voltage

Figure 5 shows the dielectric loss of PU and PU/$ZrSiO_4$ composites. In low frequency region, all the composites exhibited a decrease in loss with increase in frequency and is found to be almost stable in the range of 1 kHz –1 MHz. The high loss at low frequency is due to interfacial polarization and the subsequent increase in dielectric loss with increase in frequency is attributed to the dipolar polarization relaxation of the polymer (Variar et al., 2021). The dielectric loss of all elastomers remains low (~0.04) at 1 kHz - 1 MHz even with the increment of $ZrSiO_4$ content. This may be due to the insulative characteristics of ceramic materials possessed by $ZrSiO_4$ which exhibit low current leakage (Meena et al., 2011). This contributes to the low conductivity of the composite as well. As shown in Figure 6, the conductivity of the elastomer remains low (< $2.3X10^{-8}$ S/m) even with the increment of $ZrSiO_4$ content at 1 kHz.

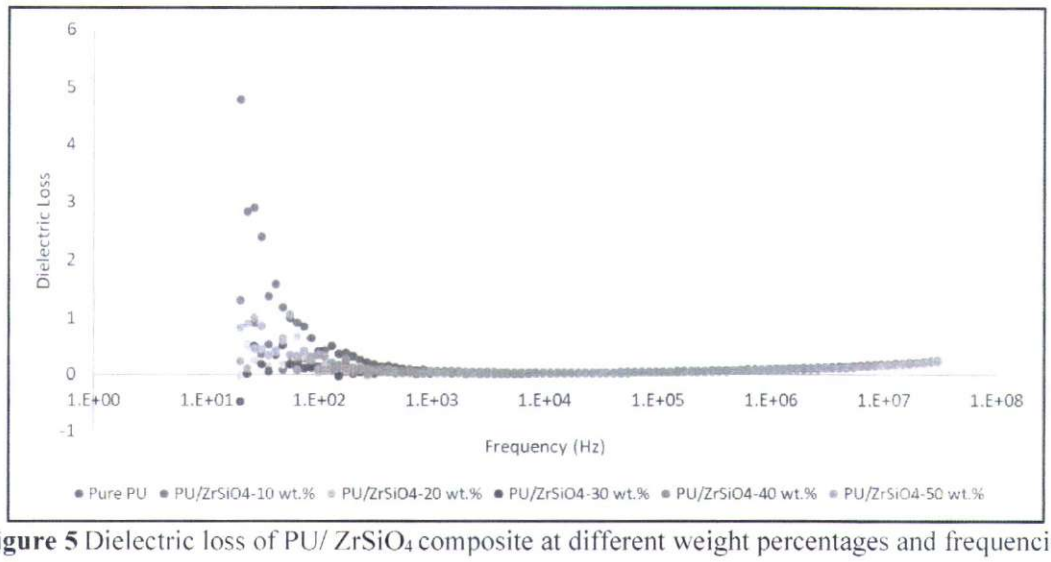

Figure 5 Dielectric loss of PU/ $ZrSiO_4$ composite at different weight percentages and frequencies

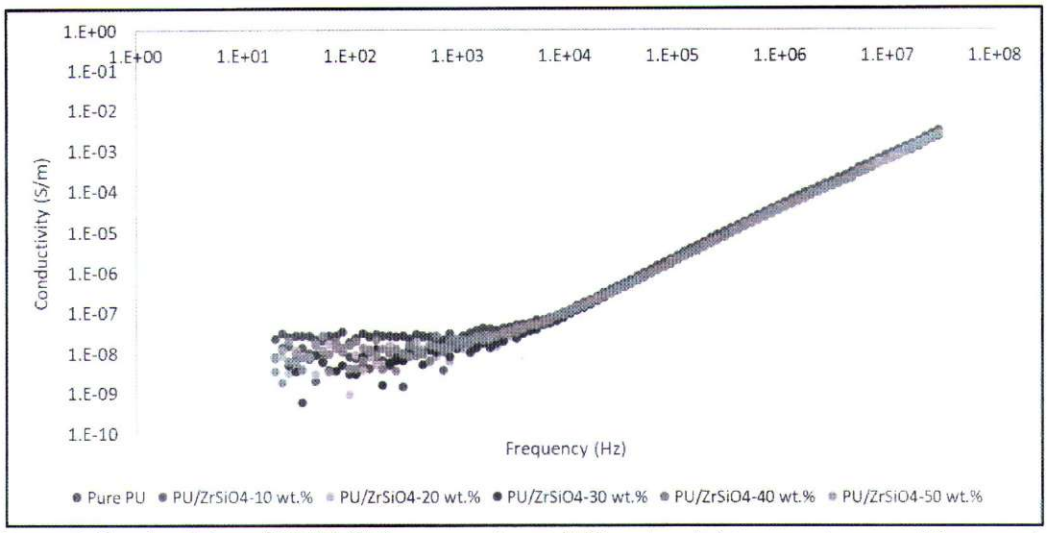

Figure 6 Conductivity of PU/$ZrSiO_4$ composite at different weight percentages and frequencies

The mechanical properties of the elastomer have a vital influence on mechano-electrical energy conversion. Figure 7(a) shows the ultimate tensile stress of PU and PU/$ZrSiO_4$ composites. By increasing the $ZrSiO_4$ filler content until 20 wt.%, the tensile strength also increased due to particle enhancement. At 20 wt.% of $ZrSiO_4$, the tensile stress of the composite reaches 6.74 MPa, which is a 122% increment. The improvement of tensile strength is attributed to the good interface between the PU matrix and $ZrSiO_4$ fillers which encourages the perfect stress transfer. Good tensile strength is strongly dependent on effective and uniform stress distribution. However, when the $ZrSiO_4$ content increases from 30 wt.% and above, the tensile strength decreases. This is due to the agglomeration of $ZrSiO_4$ filler within the PU matrix. It creates voids and acts as a flaw that limits tensile strength (Chen et al., 2014). On the other hand, the elongation of breaks of all elastomers was also investigated. Figure 7(b) shows the elongation at breaks of PU and PU/ZrSiO4 composites. The result shows that the elongation at break decreases with the increment of $ZrSiO_4$ content, indicating a change in the PU matrix from a ductile material to a more brittle composite material. However, even at 50 wt.% of $ZrSiO_4$ content, the composite still possesses high elongation at 587%.

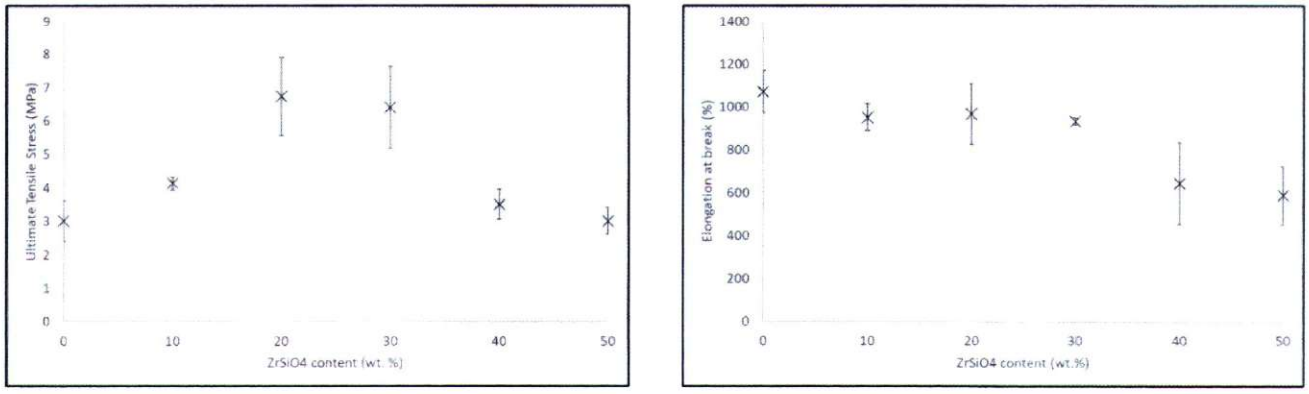

Figure 7 Mechanical characteristics of PU/$ZrSiO_4$ composites (a) ultimate tensile stress, (b) elongation at the break

The dispersion state of the $ZrSiO_4$ nanofillers within the PU matrix was further confirmed with FESEM images, as shown in Figure 8 (a-b). Figure 8(a) confirmed that the $ZrSiO_4$ nanofillers in PU/$ZrSiO_4$-20 wt.% nanocomposite exhibit a more well dispersed state where less agglomeration of nanofillers was observed, compare to PU/$ZrSiO_4$-50 wt.% nanocomposite in figure 8(b). The agglomeration of nanofillers provide a stress concentration effect and reduce the tensile strength of nanocomposite (Chee & Jawaid, 2019). Other than that, the agglomeration nucleates voids and accelerates the propagation of internal cracks, causing the reduction of ductility (Sun et al., 2020). These explained the differences in tensile strength and elongation capability between PU/$ZrSiO_4$-20 wt.% and PU/$ZrSiO_4$-50 wt.% nanocomposite. Further investigation using EDX analysis in figure 9 (a-f) shows the dispersion of ZrSiO4 nanofillers within the PU matrix. It is proven that the $ZrSiO_4$ nanofillers in PU/$ZrSiO_4$-20 wt.% nanocomposite dispersed better compare to PU/$ZrSiO_4$-20 wt.% nanocomposite, where agglomeration of nanofillers were obviously presented.

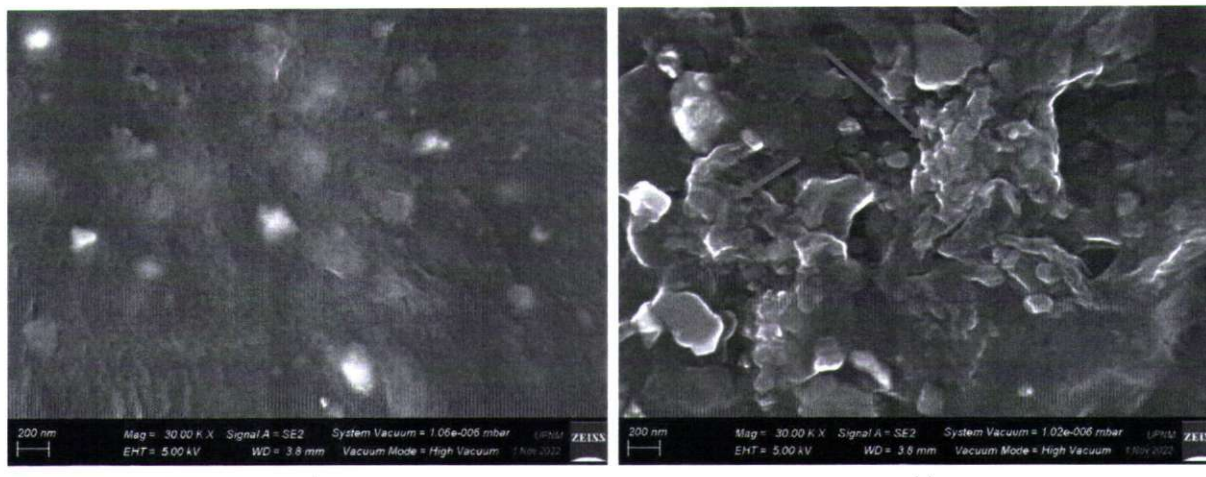

a) b)

Figure 8 FESEM images of composite: (a) PU/$ZrSiO_4$-20 wt.%; (b) PU/$ZrSiO_4$-50 wt.% (red arrows indicate the location of $ZrSiO_4$ agglomerate).

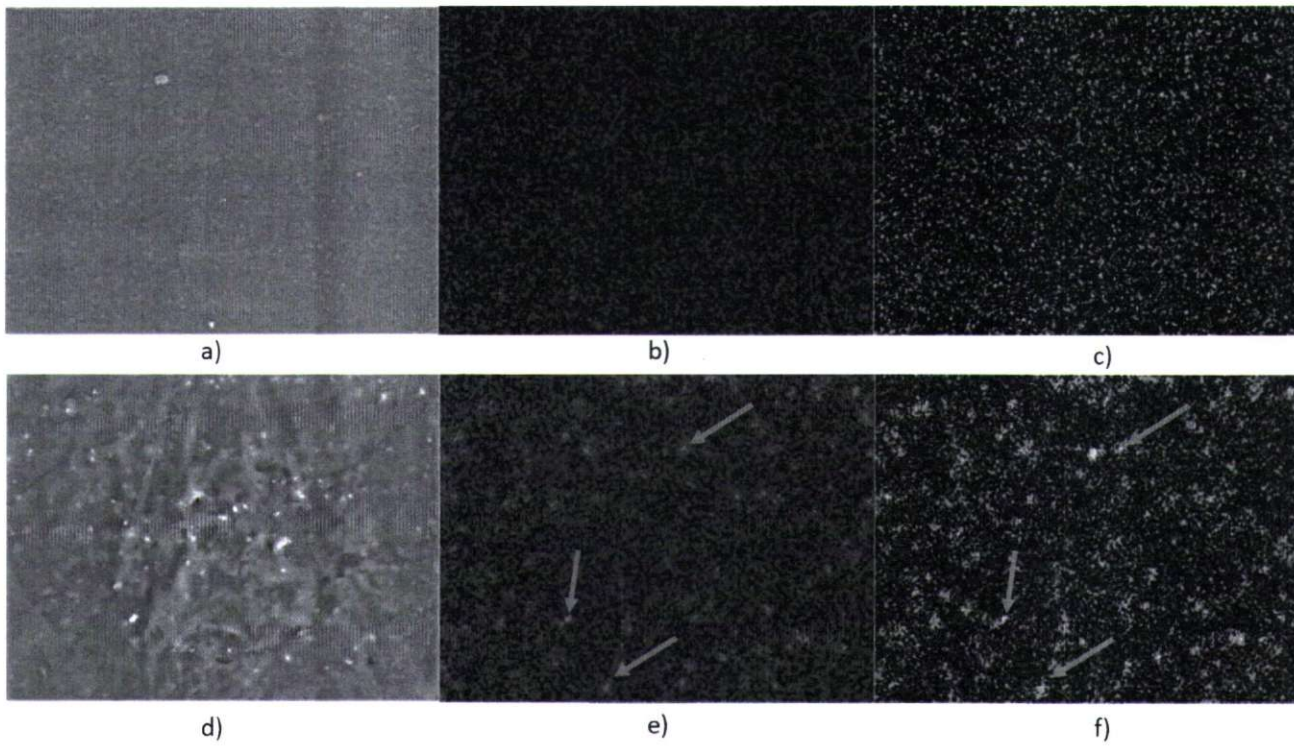

a) b) c)

d) e) f)

Figure 9 EDX mapping of nanocomposite; (a) FESEM image of PU/$ZrSiO_4$-20 wt.% composite; (b) zirconium mapping in PU/$ZrSiO_4$-20 wt.% composite; (c) silicone mapping in PU/$ZrSiO_4$-20 wt.% composite; (d) FESEM image of PU/$ZrSiO_4$-50 wt.% composite; (e) zirconium mapping in PU/$ZrSiO_4$-50 wt.% composite; (f) silicone mapping in PU/$ZrSiO_4$-20 wt.% composite. Red arrows indicate the location of $ZrSiO_4$ nanofillers agglomerate.

5. Conclusion

This study has successfully incorporated $ZrSiO_4$ with PU matrix, as demonstrated by the FTIR characterization. The presence of $ZrSiO_4$ helps in increasing the interfacial polarization with the PU matrix, which directly increases the dielectric permittivity of PU/$ZrSiO_4$ composites. Interestingly, the dielectric loss and the conductivity remain low, even at high $ZrSiO_4$ content. The mechanical characterization shows that the elongation of the composite deteriorates with the presence of $ZrSiO_4$ contents, but it still possesses high flexibility. The PU/$ZrSiO_4$ nanocomposite has promising potential for applications in the energy harvesting industry using elastomer, which requires high energy storage capability, low losses, and excellent flexibility.

Acknowledgments

The authors would like to thank the Ministry of Higher Education Malaysia and the National Defense University Malaysia for providing financial support under FRGS/1/2020/TK0/UPNM/02/10.

References

Brochu, P., & Pei, Q. (2010). Advances in Dielectric Elastomers for Actuators and Artificial Muscles. *Macromolecular Rapid Communications*, *31*(1), 10–36. https://doi.org/10.1002/marc.200900425

Chee, S. S., & Jawaid, M. (2019). *The Effect of Bi-Functionalized MMT on Morphology, Thermal Stability, Dynamic Mechanical, and Tensile Properties of Epoxy Organoclay Nanocomposites*. 18.

Chen, R. S., Ahmad, S., Ghani, M. H. A., & Salleh, M. N. (2014). *Optimization of high filler loading on tensile properties of recycled HDPE PET blends filled with rice husk*. 46–51. https://doi.org/10.1063/1.4895168

Dias, R. C. M., Góes, A. M., Serakides, R., Ayres, E., & Oréfice, R. L. (2010). Porous biodegradable polyurethane nanocomposites: Preparation, characterization, and biocompatibility tests. *Materials Research*, *13*(2), 211–218. https://doi.org/10.1590/S1516-14392010000200015

Gao, S., Zhao, H., Zhang, N., & Bai, J. (2021). Enhanced Electromechanical Property of Silicone Elastomer Composites Containing TiO2@SiO2 Core-Shell Nano-Architectures. *Polymers*, *13*(3), 368. https://doi.org/10.3390/polym13030368

He, X., Zhou, J., Jin, L., Long, X., Wu, H., Xu, L., Gong, Y., & Zhou, W. (2020). Improved Dielectric Properties of Thermoplastic Polyurethane Elastomer Filled with Core–Shell Structured PDA@TiC Particles. *Materials*, *13*(15), 3341. https://doi.org/10.3390/ma13153341

Liu, Y., Liu, L., Zhang, Z., & Leng, J. (2009). Dielectric elastomer film actuators: Characterization, experiment and analysis. *Smart Materials and Structures*, *18*(9), 095024. https://doi.org/10.1088/0964-1726/18/9/095024

Luo, Z., Zhang, L., Liang, Y., Wen, S., & Liu, L. (2022). Improved the dielectric properties of thermoplastic polyurethane elastomer filled with MXene nanosheets and BaTiO3 nanofibers. *Polymer Testing*, *111*, 107592. https://doi.org/10.1016/j.polymertesting.2022.107592

Meena, J. S., Chu, M.-C., Wu, C.-S., Ravipati, S., & Ko, F.-H. (2011). Environmentally Stable Flexible Metal-Insulator-Metal Capacitors Using Zirconium-Silicate and Hafnium-Silicate Thin Film Composite Materials as Gate Dielectrics. *Journal of Nanoscience and Nanotechnology*, *11*(8), 6858–6867. https://doi.org/10.1166/jnn.2011.4247

Musyarofah, Lestari, N. D., Nurlaila, R., & Muwwaqor, N. F. (2019). *Synthesis of high-purity zircon, zirconia, and silica nanopowders from local zircon sand*. 38.

Namitha, L. K., & Sebastian, M. T. (2017). High permittivity ceramics loaded silicone elastomer composites for flexible electronics applications. *Ceramics International*, *43*(3), 2994–3003. https://doi.org/10.1016/j.ceramint.2016.11.080

Nandiyanto, A. B. D., Oktiani, R., & Ragadhita, R. (2019). How to Read and Interpret FTIR Spectroscope of Organic Material. *Indonesian Journal of Science and Technology*, *4*(1), 97. https://doi.org/10.17509/ijost.v4i1.15806

Pelrine, R., & Kornbluh, R. (2008). INTRODUCTION: HISTORY OF DIELECTRIC ELASTOMER ACTUATORS. In *Dielectric Elastomers as Electromechanical Transducers* (pp. xi–xiii). Elsevier. https://doi.org/10.1016/B978-0-08-047488-5.00031-9

Stiubianu, G., Bele, A., Cazacu, M., Racles, C., Vlad, S., & Ignat, M. (2015). Dielectric silicone elastomers with mixed ceramic nanoparticles. *Materials Research Bulletin*, *71*, 67–74. https://doi.org/10.1016/j.materresbull.2015.07.005

Sun, Y., Zhao, Y., Wu, J., Kai, X., Zhang, Z., Fang, Z., & Xia, C. (2020). Effects of particulate agglomerated degree on deformation behaviors and mechanical properties of in-situ ZrB12/nanoparticles reinforced AA6016 matrix composites by finite element modeling. *Materials Research Express*, *7*(3), 036507. https://doi.org/10.1088/2053-1591/ab7b27

Varghese, J., Joseph, T., & Sebastian, M. T. (2011). ZrSiO4 ceramics for microwave integrated circuit applications. *Materials Letters*, *65*(7), 1092–1094. https://doi.org/10.1016/j.matlet.2011.01.020

Variar, L., Muralidharan, M. N., Narayanankutty, S. K., & Ansari, S. (2021). High dielectric constant, flexible and easy-processable calcium copper titanate/thermoplastic polyurethane (CCTO/TPU) composites through simple casting method. *Journal of Materials Science: Materials in Electronics*, *32*(5), 5908–5919. https://doi.org/10.1007/s10854-021-05311-z

Wan, W., Luo, J., Huang, C., Yang, J., Feng, Y., Yuan, W.-X., Ouyang, Y., Chen, D., & Qiu, T. (2018). Calcium copper titanate/polyurethane composite films with high dielectric constant, low dielectric loss and super flexibility. *Ceramics International*, *44*(5), 5086–5092. https://doi.org/10.1016/j.ceramint.2017.12.108

Yang, Y., Gao, Z.-S., Yang, M., Zheng, M.-S., Wang, D.-R., Zha, J.-W., Wen, Y.-Q., & Dang, Z.-M. (2019). Enhanced energy conversion efficiency in the surface modified BaTiO3 nanoparticles/polyurethane nanocomposites for potential dielectric elastomer generators. *Nano Energy*, *59*, 363–371. https://doi.org/10.1016/j.nanoen.2019.02.065

Zhang, Z., Liu, L., Fan, J., Yu, K., Liu, Y., Shi, L., & Leng, J. (2008). *New silicone dielectric elastomers with a high dielectric constant* (D. K. Lindner, Ed.; p. 692610). https://doi.org/10.1117/12.775989

Zhang, Z., Sun, S., Liu, L., Yu, K., Liu, Y., & Leng, J. (2009). *Dielectric properties of carbon nanotube/silicone elastomer composites* (J. Leng, A. K. Asundi, & W. Ecke, Eds.; p. 749315). https://doi.org/10.1117/12.845406